THREE-DIMENSIONAL NONLINEAR FINITE ELEMENT ANALYSIS ON REINFORCED CONCRETE WALLS ENHANCED BY TRANSVERSE CONFINING STEEL

N. Minami[1] and T. Nakachi[2]

[1] *Graduate Student, Dept. of Architecture and Civil Engineering, Fukui University of Technology Fukui, Japan*
[2] *Professor, Dept. of Architecture and Civil Engineering, Architecture Major, Fukui University of Technology, Fukui, Japan*
Email: nakachi@fukui-ut.ac.jp

ABSTRACT:

In high-rise reinforced concrete buildings, the edge area of wall columns and core walls with a rectangular section is subjected to high compressive stress at flexural yielding. Reinforcing this area is considered to be effective for improving the deformation capacity of the wall columns and core walls. In shear walls, reinforcing the boundary columns and panels, which are subjected to high compressive stress, effectively improves the deformation capacity of shear walls. Previously, lateral loading tests of wall columns[1)], shear walls[2)] and core walls[3)] were conducted on areas of concrete confinement of high compressive stress. This paper analyzes those lateral loading tests using the three-dimensional nonlinear finite element method (FEM), and examines the ductility of wall columns, shear walls and L-shaped core walls. The results show that reinforcing the area of high compressive stress improves the deformation capacity of these components.

KEYWORDS: FEM analysis, reinforced concrete, wall, deformation capacity, confining steel

1. INTRODUCTION

In wall columns with a rectangular section, the edge area is subjected to high compressive stress at flexural yielding. In multistory shear walls installed in high-rise buildings, the boundary columns and panels are subjected to high compressive stress at lateral loading. In a core wall system high-rise building, the center core of which consists of four L-shaped core walls, the axial load of the core wall is very high when a diagonal seismic force occurs. In particular, the corner and the area near the corner of the L-shaped core wall are subjected to high compressive stress. Reinforcing these areas of high compressive stress is considered to be effective for improving the deformation capacity of these components. This paper analyzes lateral loading tests of these components conducted previously using the three-dimensional nonlinear FEM, and examines the relationship between the degree of confinement of these areas of high compressive and the deformation capacity of these components.

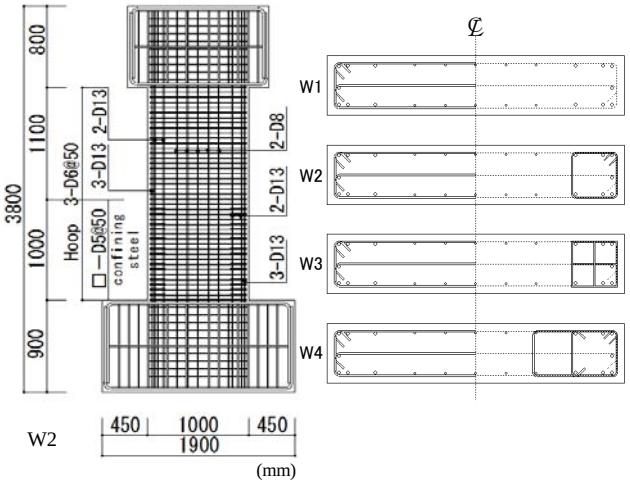

Fig. 1 Test Specimens

Table 1 Test Specimens

Specimen	W1～W4
Section b×D	200mm×1000mm
Height of Loading h	2500mm
Shear Span Ratio M/QD	2.5
Axial Stress Ratio σ_0/Fc	0.35
Main Reinf.(SD345)	14-D13,10-D8
Lateral Reinf.(SD345)	3-D6@50

2. WALL COLUMNS

2.1 Lateral Loading Test of Wall Columns

2.1.1 Test specimens

The configuration and arrangement of reinforcement in the specimens are shown in Fig. 1. Four half-scale wall column specimens were tested. Each specimen represented the wall columns of the first story of a high-rise building of approximately fifteen stories. The dimensions of the specimens and the arrangement of confining steel are shown in Table 1 and Table 2, respectively. The specified design concrete strength Fc was 24 N/mm^2. The physical properties of the concrete and reinforcement are listed in Table 3 and Table 4, respectively.

All the specimens were the flexural type. Specimen W1 had no confining reinforcement. Specimen W2 was confined at the edge area using square closed reinforcement. Specimen W3 was confined at the edge area using 田-type welded wire mesh. Specimen W4 was confined at the edge area using rectangular closed reinforcement and tie bars. The confining bars were arranged up to a height corresponding to the clear height of the first story (h: 1000 mm).

2.1.2 Test procedure

In the cyclic lateral loading tests, the specimens were subjected to forces by an actuator connected to the reaction wall. The lateral loading tests were conducted by a cantilever type. The loading was controlled by the horizontal drift angle at a height corresponding to the center level of the beam in the second floor (h: 1200 mm). The loading was cyclic lateral loading at R (drift angle) = 1.25/1000 (rad.), 2.5/1000 (1 cycle respectively), 5/1000, 10/1000, 15/1000, 20/1000, 25/1000 (2 cycles respectively), 30/1000 (1 cycle).

2.1.3 Test results

Table 2 Confining Steel

Specimen	Cofining Steel	Bar Size	Pitch (mm)	Confining Area L (mm)
W1	—	—	—	—
W2	closed(square)	D5	50	155
W3	田-welded wire mesh	5φ	50	155
W4	closed(rectangular)	D5	50	285
	tie	D5	50	—

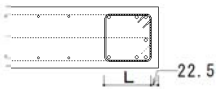

Table 3 Physical Properties of Concrete

Compressive Strength σ_B (N/mm^2)	Young's Modulus (×10^{4}N/mm^2)	Strain at Max. Stress (%)
23.0	1.90	0.24

Teble 4 Physical Properties of Steel

Bar Size	Yield Strength (N/mm^2)	Maximum Strength (N/mm^2)	Elogation (%)
5φ	501	551	13.1
D5	390	443	16.4
D6	421	559	22.3
D8	355	508	24.7
D13	375	550	25.2

Table 5 Test Results

Specimen	Maximum strength			Limit Drift Angle
	Exp. Load	Cal. Load		
		Qu1	Qu2	
	(kN)	(kN)	(kN)	(×1/1000rad.)
W1	404	434	327	16.1
W2	392	434	327	25.0
W3	418	434	327	34.5
W4	393	434	321	25.0

Calculation[4)]
・Ultimate Strength of Wall
Mu1=0.9・at・σy・D+0.45・aw・σwy・D+0.45・ND
・Ultimate Strength of Column
Mu2=0.5・ag・σy・g1・D+0.5・ND・{1-N/(B・D・Fc)}
Qu1=Mu1/h , Qu2=Mu2/h , h=2.5m

The test results are listed in Table 5. All of the main reinforcement at the tensile end yielded at approximately at R = 5/1000. At the final stage, except for Specimen W4, the specimens crumbled and could not withstand the axial load, and the strength decreased instantly.

The limit drift angle of Specimen W1, which was not confined at the edge area, was Rmax = 16.1/1000. On the other hand, the limit drift angles of Specimens W2, W3 and W4, which were confined at the edge area, were Rmax = 25/1000, 34.5/1000, 25/1000, respectively. A larger amount of confining steel had a significant effect on improving the deformation capacity of the wall columns. Comparing Specimens W2 and W4, the confining area did not have an effect on the limit drift angle.

2.2 Outline of FEM Analysis of Wall Columns

2.2.1 Analytical models and analytical procedure

The analytical models of specimens are shown in Fig. 2. The analysis was done using the three-dimensional nonlinear FEM. Every node at the bottom of wall columns was confined by a pin support. The stiffness of the top stub element was sufficiently large compared with the panel area. Concrete was represented by 8-node isoparametric solid elements. The physical properties of concrete in the experiments were used for the analytical models. The failure curve of bi-axial compression was represented by Onuma's model[5]. The compressive descending stress-strain relationships were linear. The concrete confining effect was represented by the results of compression tests which were conducted together with the lateral loading tests of the wall columns[1].

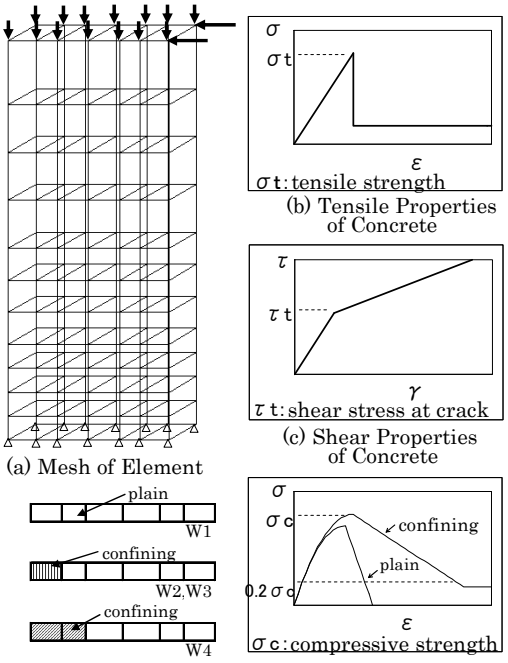

Fig. 2 Analysis Models

Cracks in concrete elements were represented by the smeared crack model. Concrete cracked when the maximum principal stress exceeded the tensile strength. After cracking, tension normal to the crack direction was cut off, and shear properties at the crack were bi-linear. The reinforcement was assumed to be a linear element, the stress-strain relationships of the reinforcement were assumed to be bilinear, and the bond between the reinforcement and concrete was assumed to be a perfect bond. The analytical models were subjected to monotonic loading, and the displacement incremental method was used. After constant axial loading, the model was loaded laterally.

2.2.2 *Analytical results*

The load-deflection curves and the test results are compared in Fig. 3. The load shows that at the loading point, and the drift angle is that at the control point of tests. In the analytical results, the limit drift angle is the drift angle when the load is less than 80% of the maximum load. The load-deflection curves are shown till the limit drift angle in the figure.

In the analytical results, the limit drift angle of Specimen W2, which was confined at the edge area, was larger than that of Specimen W1 which was not confined there. This analytical result suggests that the confining effect improved the deformation capacity of wall columns. This result matches the experimental one. The limit drift angle of Specimen W3, which had a larger amount of confining steel and was more confined, was larger than that of Specimen W2. This result suggests increased deformation capacity, and the result matches the experimental one, too. The limit

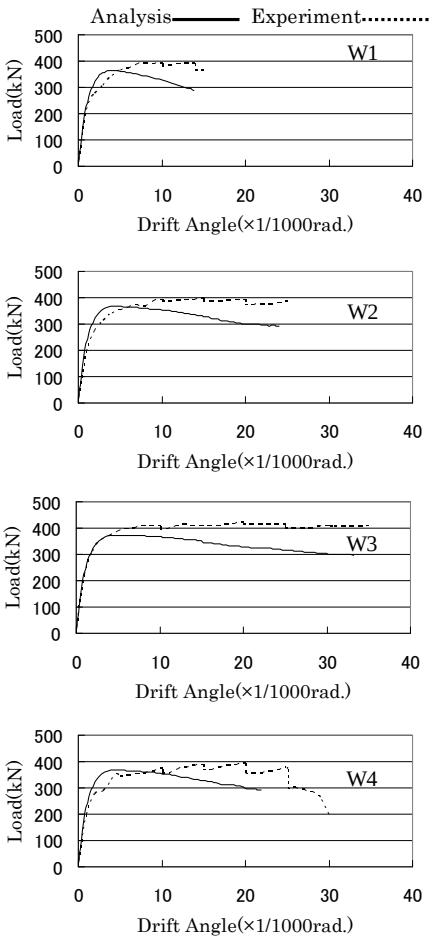

Fig. 3 Load-Deflection Curves

drift angle of Specimen W4, which had a larger confining area, was smaller than that of Specimen W2. However, in the test result, the limit drift angle of Specimens W2 and W4 was identical, that is, the analytical result did not match the experimental one. The reason is thought to be that the confining effect at the confining area of Specimen W4 was lower than that of Specimen W2 in the analysis.

Regarding the deformation capacity, the analytical results matched the experimental ones on the whole, and hence the analysis represented the concrete confining for the deformation capacity of wall columns. However, the stiffness in the analysis was larger than that in the experiment, and the maximum loads were lower than those in the experiment on the whole.

3. SHEAR WALLS

3.1 Lateral Loading Test of Shear Walls

3.1.1 Test specimens

The configurations and dimensions of the specimens are shown in Fig. 4. Five one-fifth-scale shear wall specimens were tested. Each of the specimens represented the shear walls of the lower three stories in a building of approximately thirty stories. The physical properties of the concrete and the reinforcement are listed in Tables 6 and 7, respectively. Specimen S1 was designed to have a low transverse reinforcement ratio of 0.2% in the boundary columns while S2 had a high transverse reinforcement ratio of 0.7%. Specimen S3 was designed to have a high wall horizontal reinforcement ratio of 1.2%. This contrasts with Specimen S2's horizontal reinforcement ratio of 0.7%. Specimens S4 and S5 were confined at the first story of the panel using tie bars and closed reinforcement, respectively.

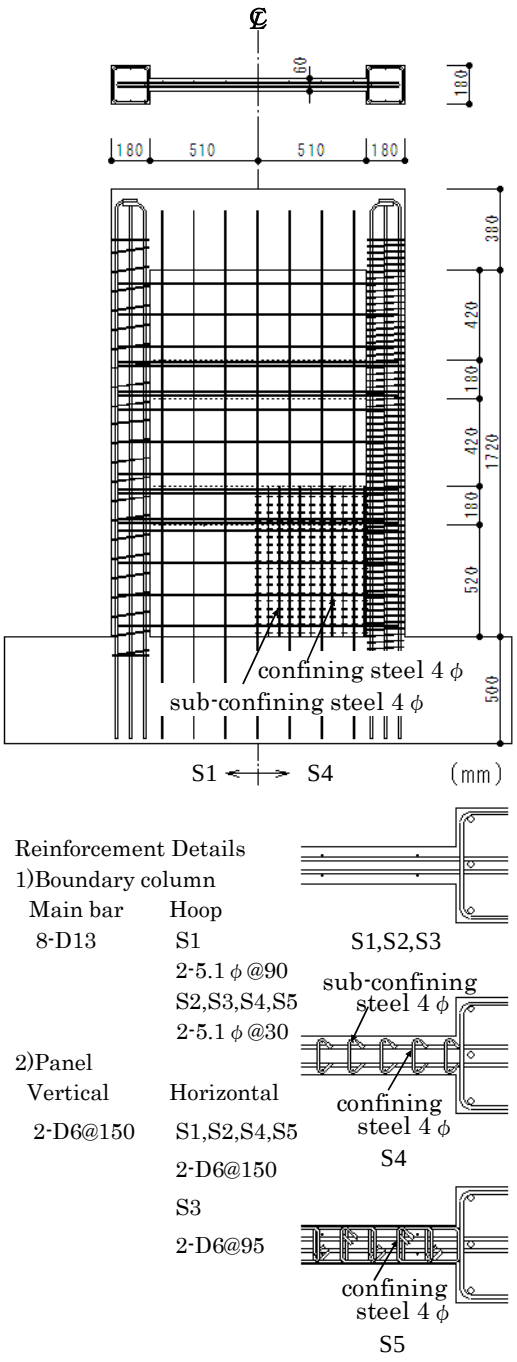

Fig. 4 Test Specimens

3.1.2 Test procedure

In the cyclic lateral loading tests, the specimens were subjected to forces by an actuator connected to the reaction wall. The lateral loading tests were conducted by a cantilever type. A constant axial loading force of 9.8 N/mm^2 was applied to each boundary column. The added moment was loaded in proportion to the lateral loading in order to maintain a constant shear span ratio (2) at the bottom of the shear wall. Two actuators were vertically connected to the reaction frame to achieve this. The loading was controlled by the horizontal drift angle at the first story (h: 700 mm). The loading was cyclic lateral loading at R = 1/1000 (1 cycle), 2/1000, 5/1000, 7.5/1000, 10/1000, 15/1000 (2 cycles respectively), and 20/1000 (1 cycle).

3.1.3 Test results

The test results are listed in Table 8. In every test, the panel vertical reinforcement and the boundary column main reinforcement yielded. The bottom of the boundary column on the side being compressed also appeared to crumble a little during this time. The load of Specimen S1 decreased rapidly during the second cycle of 15/1000 due to the concrete at the bottom of the boundary column and the panel being crushed. The load of Specimen S2 decreased after it had exceeded 15/1000. This was due to the bottom panel slipping and no crumbling occurred. Specimens S3, S4 and S5 withstood most of the maximum loads until 40/1000. At the final stage, S3 crumbled in the compressive region at the bottom of the panel. S5 slipped at the bottom of the panel.

Table 6 Physical Properties of Concrete

Specimen	Compressive Strength σ_B (N/mm^2)	Young's Modulus ($\times 10^4 N/mm^2$)	Sprit Strength (N/mm^2)
S1	37.4	2.95	-
S2	38.1	2.55	-
S3	39.2	2.95	2.3
S4	40.5	2.99	2.4
S5	41.0	2.95	2.9

Table 7 Physical Properties of Steel

Bar Size		Yield Strength (N/mm^2)	Maximum Strength ($N/mm2$)	Young's Modulus ($\times 10^5 N/mm^2$)	Elongation (%)
4φ	(S3,S4,S5)	987.9	1450.5	1.95	5.5
5.1 φ	(S1,S2)	1388.4	1483.7	2.13	11.4
5.1 φ	(S3,S4,S5)	1334.8	1413.9	2.01	8.7
D6	(S1,S2)	367.5	508.3	1.79	14.1
D6	(S3,S4,S5)	402.2	521.3	1.83	25.2
D13	(S1,S2)	378.1	550.0	1.89	18.8
D13	(S3,S4,S5)	362.7	526.3	2.02	19.2

Table 8 Test Results

Specimen	Maximun Strength		Limit Drift Angle
	Exp.Load (kN)	Cal.Load (kN)	(×1/1000rad.)
S1	402	407	15.8
S2	414	407	16.5
S3	416	403	38.3
S4	404	403	>40.0
S5	397	404	>40.0

Calculation[4)]

$Mu=0.9at\cdot\sigma y\cdot D+0.4\cdot aw\cdot\sigma wy\cdot D+0.5\cdot ND\cdot\{1-N/(Bc\cdot D\cdot Fc)\}$

3.2 Outline of FEM Analysis of Shear Walls

3.2.1 Analytical models and analytical procedure

The analytical models of specimens are shown in Fig. 5. The analysis was done using the three-dimensional nonlinear FEM as in the case of wall columns. The concrete confining effect was represented by the results of compression tests which were conducted together with the lateral loading tests of the shear walls [2)]. The analytical models were loaded laterally after constant axial loading as in the case of wall columns.

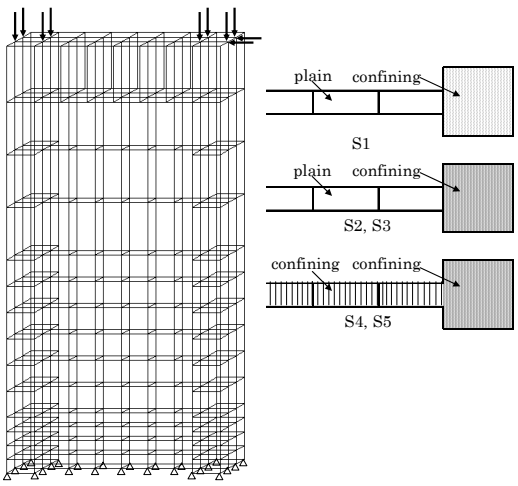

Fig. 5 Analysis Models

3.2.2 Analytical results

The load-deflection curves and the test results are compared in Fig. 6. The load shows that at the loading point, and the drift angle is that at the first story (h: 700 mm). In the analytical results, the limit drift angle of Specimen S1, which was designed to have a low transverse reinforcement ratio of the boundary columns, was smaller than that of Specimen S2 which was the standard specimen. This analytical result suggests that the decrease of the confining effect reduced the compressive ductility of the boundary columns and reduced the deformation capacity of Specimen S1. This result matches the experimental one. The limit drift angle of Specimen S3, which was designed to have a high wall horizontal reinforcement ratio, was larger than that of Specimen S2, and the decrease of the load did not occur until R = 40/1000. This result suggests that the increase of the wall horizontal reinforcement ratio improved the ratio of the shear strength to the flexural strength and improved the deformation capacity of Specimen S3. This result almost matches the experimental one, too. The limit drift angles of Specimens S4 and S5, which were confined at the first story of the panel using tie bars and closed reinforcement, were larger than that of Specimen S2, and the decrease of the load did not occur until the final stage. This

analytical result suggests that the confining effect of the panel concrete improved the compressive ductility of that area and improved the deformation capacity of Specimens S4 and S5. This result matches the experimental one. Regarding the deformation capacity, the analytical results matched the experimental ones on the whole, and the analysis represented the concrete confining effect for the deformation capacity of shear walls.

4. CORE WALLS

4.1 Lateral Loading Test of Core Walls

4.1.1 Test specimens

The configuration and arrangement of reinforcing in the specimens are shown in Fig. 7. Four one-eighth-scale core wall specimens were tested. Each specimen represented the core walls of the lower three stories of a high-rise building of approximately twenty-five stories. The specimens had a shear span ratio of 2.5. The specified design concrete strength was 588 N/mm^2. The physical properties of the concrete and reinforcement are listed in Tables 9 and 10, respectively. All of the specimens were the flexural type. Specimen L1 had no confining reinforcement. Specimen L2 was confined at the corner using square closed reinforcement. Specimens L3 and L4 were confined at the area near the corner using tie bars. Specimen L4 had twice the number of tie bars as Specimen L3. The confining bars were arranged up to a height corresponding to the second floor level (h: 615 mm).

4.1.2 Test procedure

In the cyclic lateral loading tests, the specimens were subjected to forces by an actuator connected to the reaction wall. A constant axial loading force was applied by a hydraulic jack over the specimen to represent the axial stress in the stage of coupling beam yielding at the center core. The axial stress was 60% of the concrete compressive cylinder strength at the positive loading for which the corner area is compressive, and 78.5 kN at the negative loading respectively. The loading was controlled by the horizontal drift angle at a height corresponding to the second floor level (h: 615 mm). The loading was cyclic lateral loading at R = 1/1000 (1 cycle), 2/1000 (2 cycle), 5/1000, 7.5/1000, and 10/1000 (1 cycle respectively).

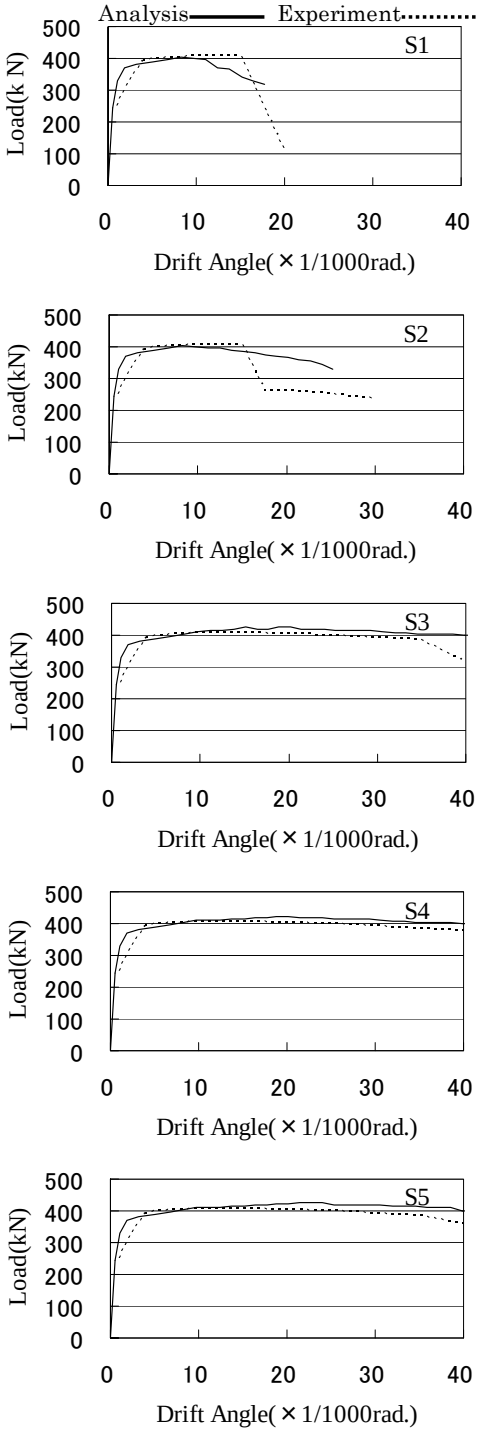

Fig. 6 Load-Deflection Curves

Table 9 Physical Properties of Concrete

Specimen	Compressive Strength σ_B (N/mm^2)	Young's Modulus (×10^{4}N/mm^2)	Sprit Strength (N/mm^2)
L1	52.6	2.97	3.74
L2	71.9	3.52	4.51
L3	70.9	3.40	4.82
L4	66.2	3.52	3.31

4.1.3 Test results

The test results are listed in Table 11. In Table 11, the maximum strengths represent values at positive loadings. At the positive loadings of all specimens, the longitudinal reinforcement at the compressive end yielded at cycle R = 1/1000. At the final stage, all specimens crumbled and the strength decreased at the positive loadings. In the case of specimens with confining reinforcement, the limit drift angle of specimens L3 and L4 which were confined at the corner and the area near the corner was larger than that of Specimen L2, which was confined at the corner only. The limit drift angle of Specimen L4, which had more confining reinforcement than Specimen L3, was larger than that of Specimen L3. These results show the effectiveness of concrete confinement. The drift angle of Specimen L1, which had no confining reinforcement, was larger than that of Specimen L2 which had confining reinforcement at the corner. The reason for these results is believed to be that the axial load of Specimen L1 was lower than that of the other specimens.

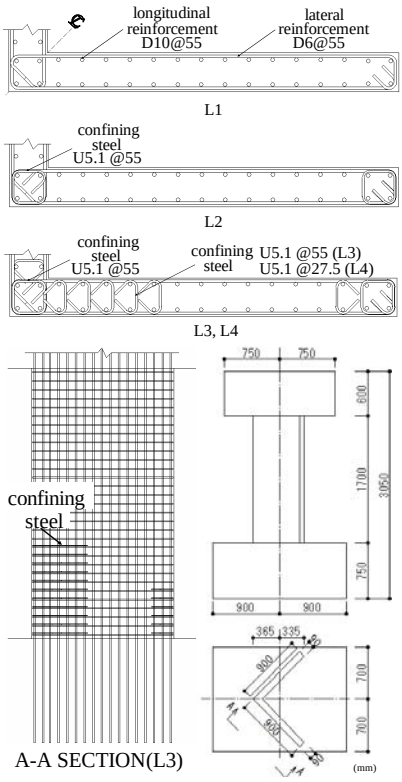

Fig. 7 Test Specimens

4.2 Outline of FEM Analysis of Core Walls

4.2.1 Analytical models and analytical procedure

The analytical models of specimens are shown in Fig. 8. The analysis was done using the three-dimensional nonlinear FEM as in the case of wall columns and shear walls. The concrete confining effect was represented by the results of compression tests which were conducted together with the lateral loading tests of the core walls [3]. The analytical models were loaded laterally after constant axial loading as in the case of wall columns and shear walls.

Table 10 Physical Properties of Steel

Bar Size	Yield Strength (N/mm^2)	Maximum Strength (N/mm^2)	Young's Modulus ($\times 10^5 N/mm^2$)	Elogation (%)
D10	360.7	518.9	1.85	18.2
D6	381.4	524.9	1.90	20.9
U5.1	1314.6	1397.5	1.91	7.5

Table 11 Test Results

Specimen	Maximun Strength		Limit Drift Angle
	Exp.Load (kN)	Cal.Load (kN)	(×1/1000rad.)
L1	464	362	4.6
L2	377	440	3.1
L3	489	436	6.0
L4	557	417	9.6

Calculation[4]

$$Mu=\{0.5\cdot ag\cdot \sigma y\cdot g1\cdot D+0.024\cdot(1+g1)(3.6-g1)\cdot b\cdot D^2\cdot Fc\}\cdot\{(Nmax-N)/(Nmax-Nb)\}$$

4.2.2 Analytical results

The load-deflection curves and the test results are compared in Fig. 9. The load shows that at the loading point, and the drift angle is that at the control point of tests. In the analytical results, the limit drift angle of Specimen L3, which was confined at the corner and the area near the corner, was larger than that of Specimen L2 which was confined at the corner only. This analytical result suggests that the increased confining area improved the deformation capacity of the core wall. This result matches the experimental one. The limit drift angle of Specimen L4, which had twice the amount of confining steel in the area near the corner compared with Specimen L3, was larger than that of Specimen L3. This result suggests the effectiveness of more confining steel, a result that matches the experimental one. The limit drift angle of Specimen L1, which had smaller concrete strength than the other specimens, was larger than that of Specimen L2. This result matches the experimental one.

Regarding the deformation capacity, the analytical results matched the experimental ones on the whole, and hence the analysis represented the concrete confining effect for the deformation capacity of core walls. However, the stiffness in the analysis was larger than that in the experiment, and the

maximum load of Specimen L4 in the analysis was lower than that in the experiment.

5. CONCLUSIONS

Lateral loading tests of reinforced concrete wall columns, shear walls and core walls were analyzed using the three-dimensional nonlinear finite element method, and the ductility of these components was compared with the experimental results. By representing the concrete confining effect in concrete elements, the analysis represented the confining effect for the deformation capacity of these components from load-deflection curves as follows:

(1) The increase of limit drift angle by confining high compressive stress area over the level in the case with no confinement, matched the experimental results.

(2) The increase of limit drift angle by greater confinement matched the experimental results.

(3) In the experimental results of core walls, the limit drift angle increased by extending the confining area. The analysis approximately matched the experimental results.

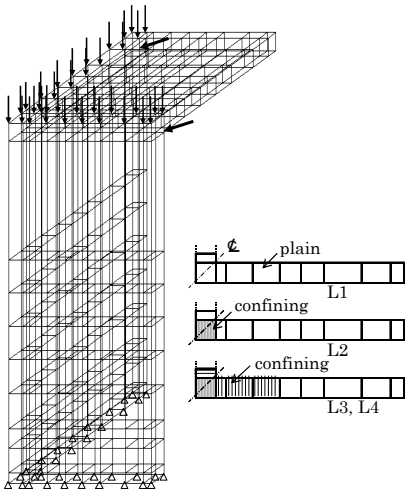

Fig. 8 Analysis Models

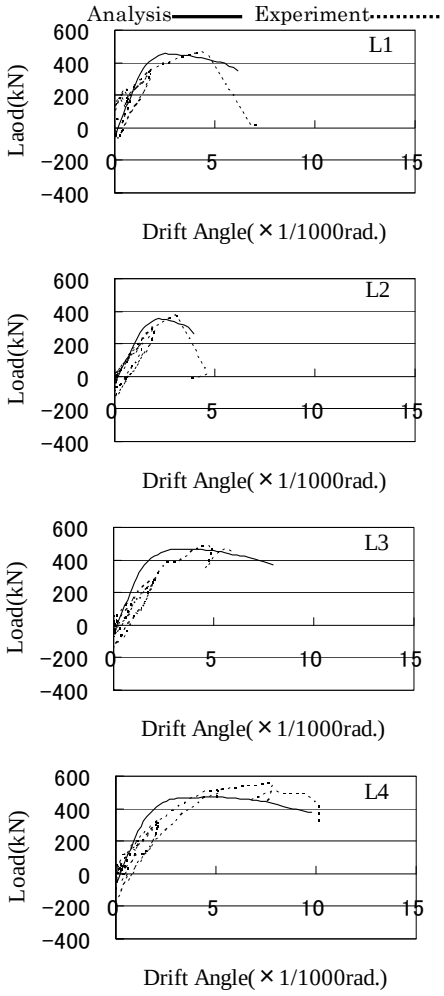

Fig. 9 Load-Deflection curves

ACKNOWLEDGMENTS

This work was supported by the FUT Research Promotion Fund. The authors are grateful for the support.

REFERENCES

1) Hiraishi, H., Teshigawara, M., Kawashima, T., Nakachi, T., et al. (1988). Experimental Study on Deformation Capacity of Wall Columns after Flexural Yielding. *Proceedings of Ninth World Conference on Earthquake Engineering* **Vol. IV,** 383–388.
2) Nakachi, T., Toda, T. and Makita, T. (1992). Experimental Study on Deformation Capacity of Reinforced Concrete Shear Walls After Flexural Yielding. *Proceedings of Tenth World Conference on Earthquake Engineering*, 3231-3236.
3) Nakachi, T., Toda, T. and Tabata, K. (1996). Experimental Study on Deformation Capacity of Reinforced Concrete Core Walls After Flexural Yielding. *Proceedings of Eleventh World Conference on Earthquake Engineering*, Paper No. 1714.
4) AIJ. (1990). Ultimate Strength and Deformation Capacity of Buildings in Seismic Design, Gihodo Shuppan.
5) JSCE. (1981). New Civil Engineering Series 29, Gihodo Shuppan.